Redox Biology 26 (2019) 101296

Contents lists available at ScienceDirect

Redox Biology

journal homepage: www.elsevier.com/locate/redox

Research Paper

A conserved motif liganding the [4Fe–4S] cluster in [4Fe–4S] fumarases prevents irreversible inactivation of the enzyme during hydrogen peroxide stress

Zheng Lu[a,*], James A. Imlay[b]

[a] Department of Biology, Guangdong Provincial Key Laboratory of Marine Biotechnology, STU-UNIVPM Joint Algal Research Center, Shantou University, Shantou, 515063, China

[b] Department of Microbiology, University of Illinois, 601 S. Goodwin Ave., Urbana, IL, 61801, USA

ARTICLE INFO

Keywords:
4Fe–4S] fumarase
Hydrogen peroxide
Irreversible damage
Bacteroides

ABSTRACT

Organisms have evolved two different classes of the ubiquitous enzyme fumarase: the [4Fe–4S] cluster-containing class I enzymes are oxidant-sensitive, whereas the class II enzymes are iron-free and therefore oxidant-resistant. When hydrogen peroxide (H_2O_2) attacks the most-studied [4Fe–4S] fumarases, only the cluster is damaged, and thus the cell can rapidly repair the enzyme. However, this study shows that when elevated levels of H_2O_2 oxidized the class I fumarase of the obligate anaerobe *Bacteroides thetaiotaomicron* (Bt-Fum), a hydroxyl-like radical species was produced that caused irreversible covalent damage to the polypeptide. Unlike the fumarase of oxygen-tolerant bacteria, Bt-Fum lacks a key cysteine residue in the typical "CX_nCX_2C″ motif that ligands [4Fe–4S] clusters. Consequently H_2O_2 can access and oxidize an iron atom other than the catalytic one in its cluster. Phylogenetic analysis showed that certain clades of bacteria may have evolved the full "CX_nCX_2C″ motif to shield the [4Fe–4S] cluster of fumarase. This effect was reproduced by the construction of a chimeric enzyme. These data demonstrate the irreversible oxidation of Fe–S cluster enzymes and may recapitulate evolutionary steps that occurred when microorganisms originally confronted oxidizing environments. It is also suggested that, if H_2O_2 is generated within the colon as a consequence of inflammation or the action of lactic acid bacteria, the inactivation of fumarase could potentially impair the central fermentation pathway of *Bacteroides* species and contribute to gut dysbiosis.

1. Introduction

Iron-sulfur ([Fe–S]) clusters are inorganic compounds containing Fe^{2+} and sulfur (S^{2-}). They are one of the most ancient types of prosthetic groups and are wide-spread in all prokaryotic and eukaryotic cells, executing diverse functions [1–4].

Iron-sulfur clusters are the traces of biological evolution in the early anaerobic earth. Their biosynthesis and assembly system were not challenged by the environment until photosynthesis eventually changed the atmospheric environment into an oxic state [5–8]. This event posed a crisis for [Fe–S] clusters: oxygen (O_2) molecules are small and non-polar, and they can quickly penetrate into microorganisms and produce highly oxidative reactive oxygen species (ROS) such as superoxide (O_2^-) and hydrogen peroxide (H_2O_2) [9–11]. These ROS can rapidly oxidize reduced iron atoms. Most [Fe–S] proteins wrap their clusters inside polypeptide, preventing ROS molecules from contacting the clusters and thereby shielding the clusters from damage. However, a small number of proteins employ clusters that are exposed to the external environment in order to bind substrates. This arrangement gives ROS the opportunity to oxidize them. Dehydratases that contain [4Fe–4S] clusters, such as fumarase, aconitase and isopropylmalate isomerase (IPMI), are such proteins [12–15].

In most [4Fe–4S] dehydratases, three of the four iron atoms in the cluster are bound to the protein skeleton through the thiol groups of cysteines; one iron atom is solvent-exposed and coordinates the substrate as a Lewis acid [6,12,16]. The three cysteine residues that bind the non-catalytic iron atoms form a specific structural motif "C-Xn-C-X_2-C" (C is cysteine; X is an arbitrary residue; n is a variable number), which is conserved in many [4Fe–4S] dehydratase sequences [6,12]. Among the four iron atoms in these well-studied [4Fe–4S] clusters, only the solvent-exposed atom is the site of ROS oxidation. ROS oxidize the [4Fe–4S] cluster, the cluster degrades, releasing the catalytic iron atom, and the enzyme loses the activity [9].

Different ROS molecules oxidize [4Fe–4S] clusters through different

* Corresponding author.
E-mail address: lzheng09@stu.edu.cn (Z. Lu).

https://doi.org/10.1016/j.redox.2019.101296
Received 22 June 2019; Received in revised form 4 August 2019; Accepted 7 August 2019
Available online 23 August 2019

mechanisms. Univalent oxidation by O_2^- converts the active $[4Fe–4S]^{2+}$ cluster to an unstable $[4Fe–4S]^{3+}$ species, which then releases Fe^{2+}. Like O_2^-, H_2O_2 also attacks the catalytic iron atom of the cluster [9,17]. However, an important difference exists here. When H_2O_2 oxidizes iron atoms (the Fenton reaction), a ferryl radical ($[FeO]^{2+}$) is initially formed [17]; it can then decompose into a into a hydroxyl radical (HO•) too:

$$Fe^{2+} + H_2O_2 \rightarrow [FeO]^{2+} + H_2O \quad (1)$$

$$[FeO]^{2+} + H^+ \rightarrow Fe^{3+} + HO\bullet \quad (2)$$

Both radicals are powerful oxidants. The highly reactive HO• has been more extensively studied; it reacts with amino acids at nearly diffusion-limited rates and can produce carbonylated sites on proteins [17]. If such damage occurred within the active site when dehydratases [4Fe–4S] clusters are oxidized by H_2O_2, the resultant damage would be irreversible. But in fact these enzymes can be fully reactivated in vitro and in vivo after being oxidized by this oxidant, indicating that the $[FeO]^{2+}$ that is produced does not oxidize the polypeptide and that aggressive HO• is not released [9,12,18]. Further analysis indicated that the nascent $[FeO]^{2+}$ pulls a second electron from the iron-sulfur cluster itself, preempting the release of a hydroxyl radical and thereby avoiding the oxidation of residues [9,15,18,19].

Bacteroides species are Gram-negative obligate anaerobes. They are among the most prominent symbionts in the human gastrointestinal tract [20–22]. In the genus, fumarase is a key [4Fe–4S] dehydratase dehydrating malate to fumarate and playing a critical role in its central succinate/propionate fermentation pathway [23,24]. In this study, we found that the fumarase from *Bacteroides thetaiotaomicron* (*B. thetaiotaomicron*) VPI-5482 surprisingly cannot be fully reactivated after it is oxidized in vitro by elevated levels of H_2O_2. In contrast it can be repaired after oxidation by either O_2^- or ferricyanide ($K_3Fe(CN)_6$). Protein carbonylation assays showed that H_2O_2 treatment carbonylated the peptide chain, suggesting that a radical species ($[FeO]^{2+}$ or HO•) is produced in the reaction and that species oxidizes the protein backbone. This is an unprecedented observation. Further tests showed that the conventional motif liganding [4Fe–4S] in dehydratases can protect peptide chains from carbonylation. This study may indicate that some bacteria evolved a modified form of [4Fe–4S] fumarase to enhance their resistance to oxidative environments.

2. Results

2.1. Bt-Fum activity cannot be fully restored after in vitro treatment with excess H_2O_2

The model bacterium *E. coli* accumulates ~ 1 μM H_2O_2 in a mutant lacking catalases and peroxidases (denoted Hpx^-) [25]. This apt dose is enough to create substantial damage to select intracellular enzymes and to DNA, and it triggers the activation of OxyR regulon, the natural mechanism by which the cell senses threatening levels of H_2O_2. Therefore, in previous investigations micromolar H_2O_2 proved useful in studying mechanisms of enzyme damage in vitro, and higher doses were seldom used [26,27].

In this study, when slightly higher concentrations of H_2O_2 (> 50 μM) were chosen to treat fumarase in vitro, Bt-Fum behaved surprisingly differently than the *E. coli* fumarase (Ec-Fum) (Fig. 1A and B). The activity of the oxidized Ec-Fum was fully restored by the addition of Fe^{2+} and dithiothreitol (DTT) in an anoxic reaction, which mirrored the results of previous investigations: the damaged [Fe–S] clusters of well-studied dehydratases can be fully repaired in vitro [19,28,29]. In contrast, the activity of Bt-Fum was only partially regained (30%–55%). We considered that when oxidized dehydratases are incubated for extended time, the damaged clusters sometimes degrade beyond the [3Fe–4S] + state, forming [2Fe–2S] clusters or even iron-free apoprotein. Such enzymes can be repaired if the cluster is rebuilt using ferrous iron plus IscS protein and cysteine to provide the sulfur atoms necessary for cluster scaffolding [19,30]. However, when cysteine and purified IscS protein were included in the reactivating reaction for oxidized Bt-Fum, they did not restore activity (Fig. 1B). This result persisted when a variety of IscS concentrations and reactivation times were employed (Fig. S1). Control experiments confirmed that IscS is competent to assemble active clusters in un-oxidized Bt-Fum apoprotein (Fig. S1); therefore, its failure to restore activity to the oxidized holoenzyme suggested that the enzyme had suffered an injury apart from cluster disintegration.

Potent oxidants other than H_2O_2—such as $K_3Fe(CN)_6$, O_2^- and molecular O_2—were also used to treat Bt-Fum. The enzyme lost activity, as expected; interestingly, in contrast to the H_2O_2 case, subsequent treatment was able to fully reactivate the enzyme (Fig. 1B, C, D). This result is also observed when Ec-Fum is treated by non-H_2O_2 oxidants [19,31,32].

Electron paramagnetic resonance (EPR) spectroscopy was performed to further check the status of the enzyme cluster after exposure to 30–100 μM H_2O_2. The ROS − damaged cluster of Ec-Fum(A) exhibited an EPR spectrum that is typical of the $[3Fe–4S]^+$ form (Fig. 2), as reported before [32]. Bt-Fum treated with 100 μM H_2O_2 generated a similar EPR signal (Fig. 2), indicating the oxidized cluster of Bt-Fum is in $[3Fe–4S]^+$ state, at least in part.

In contrast to the *B. thetaiotaomicron* fumarase, the IPMI from the same organism could be fully repaired after treatment with 100 μM H_2O_2 (Fig. S2). Thus, the irreversibility of damage is not a trait of all the *B. thetaiotaomicron* dehydratases. Further, when Bt-Fum was exposed to low intensity H_2O_2 treatment (1 μM for 20 min), it could be fully repaired (Fig. S3).

2.2. H_2O_2 − treated Bt-Fum cannot be completely reactivated in vivo

To determine the potential relevance of this phenomenon, we examined the ability of cells to repair Bt-Fum after H_2O_2 exposure occurred in vivo. The Ec-Fum(A) and Bt-Fum were expressed in an *E. coli* strain (SJ54) that lack fumarases and H_2O_2 − scavenging enzymes. Both enzymes lost activity when the bacteria were exposed to 100 μM H_2O_2. The H_2O_2 exposure was ended by the addition of catalase, and chloramphenicol was added to block the further protein synthesis. During the subsequent incubation period, the Ec-Fum(A) activity completely rebounded, but the Bt-Fum activity did not (Fig. 3). To exclude the possibility that the *E. coli* Fe–S cluster repair system doesn't work on Bt-Fum, the similar experiment was conducted with the analogous *B. thetaiotaomicron* strain (SM135). When these cells were exposed to 100 μM H_2O_2, Bt-Fum lost activity inside cells. Less than 30% of the initial activity was restored when the oxidative stress was quenched and the cells were incubated in the presence of chloramphenicol (Fig. 3). These results demonstrated that when Bt-Fum is damaged by this dose of H_2O_2, it cannot be fully repaired inside cells, consistent with the in vitro observations.

2.3. Why does excess H_2O_2 oxidation block the reactivation of Bt-Fum?

A potential explanation for the irreversible damage was that H_2O_2 might directly oxidize residues of the Bt-Fum protein. To test this possibility, Bt-Fum was overexpressed from a T7 promoter, which ensured that it was mostly in the apoprotein form, as cluster-assembly processes cannot keep up with the rate of protein synthesis. The protein was purified and further held in ice for one week in the presence of 0.5 mM EDTA, to ensure that any residual was disassembled, leaving all the protein in apo form. Assays confirmed the absence of activity. The apo-enzyme was then treated with H_2O_2. It was found that this treatment did not diminish our ability to activate the enzyme with IscS/cysteine and iron in vitro (Fig. 4). This result indicates that H_2O_2 cannot damage the peptide without the cluster, and it indirectly demonstrates that the irreversible damage observed with holoenzyme originates from

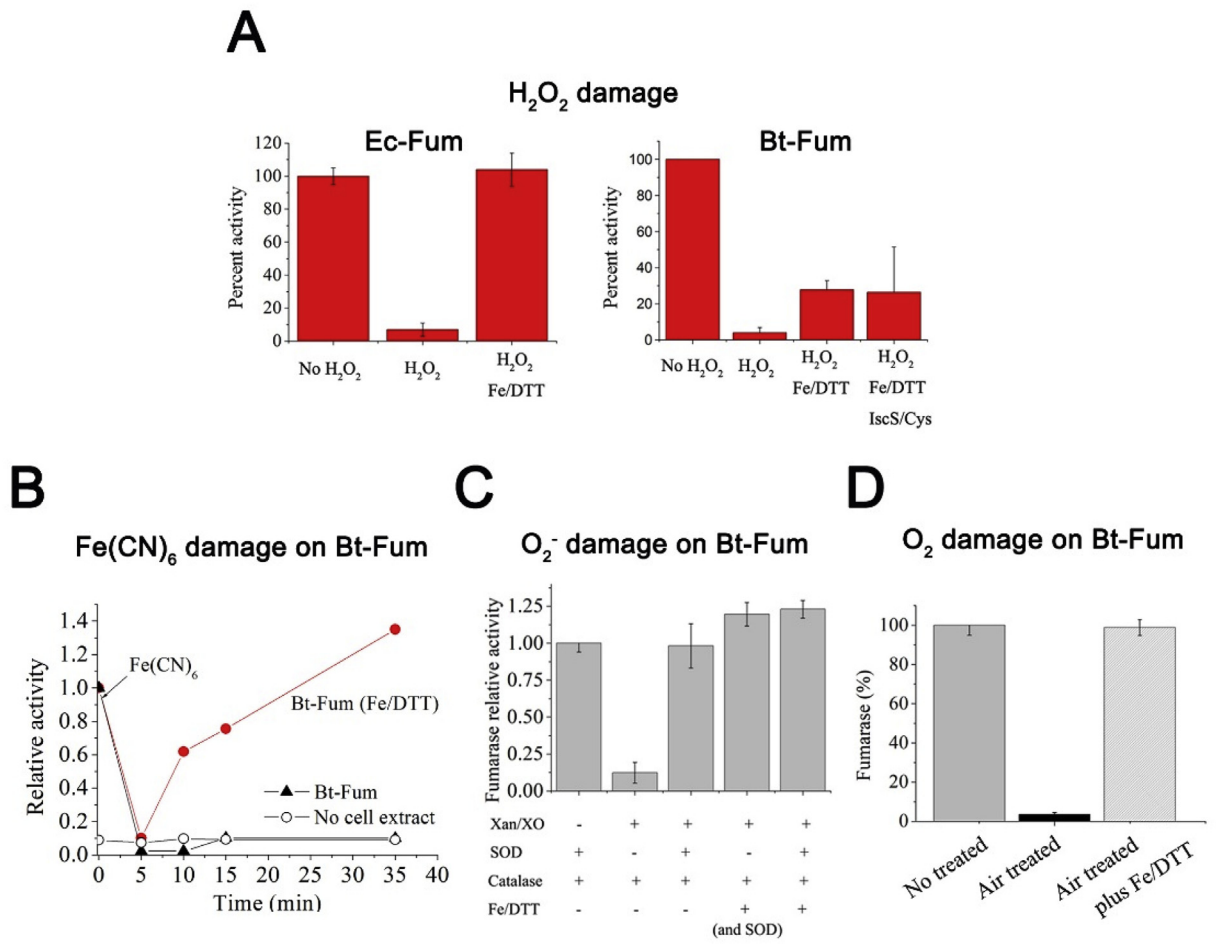

Fig. 1. Bt-Fum is irreversibly damaged by H_2O_2 but reversibly damaged by other oxidants. (A) In vitro recovery after H_2O_2 (100 μM) damage of Ec-Fum or Bt-Fum. Crude extracts were anaerobically prepared from *E. coli* or *B. thetaiotaomicron* Hpx$^-$ strains (LC106/SM135), and they were exposed to 100 μM H_2O_2 at room temperature for 5 min in an anaerobic chamber. Catalase (200 U/ml) was added to terminate H_2O_2 stress. Oxidized fumarase was then treated with $Fe(NH_4)_2(SO_4)_2$ and DTT and, where indicated, cysteine and purified *E. coli* IscS. (B–D) Damages on Bt-Fum from other oxidants: (B) $K_3Fe(CN)_6$ (100 μM), (C) O_2^- damage created by xanthine/xanthine oxidase and (D) molecular O_2 in air-saturated buffer, as described in Materials and methods.

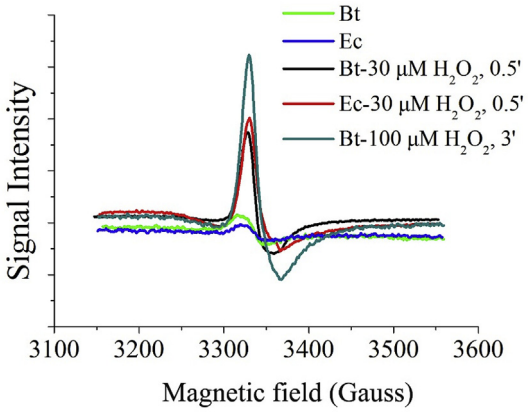

Fig. 2. After H_2O_2 treatment the iron-sulfur cluster of purified Bt-fum shows the EPR signal of a [3Fe–4S]$^+$ cluster, indicating loss of one iron atom. Purified Ec-Fum (5 μM) or Bt-Fum (5–8 μM) was inactivated by H_2O_2 in NaPi buffer (pH 7.2). Catalase was added after the treatment, and the reaction mixture was then frozen for EPR measurement.

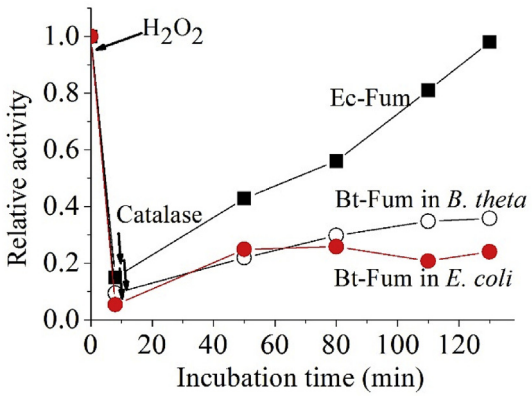

Fig. 3. H_2O_2 (100 μM) generates irreversible damage on Bt-Fum but not Ec-Fum inside living cells. *E. coli* SJ54 cells expressing Ec-Fum or Bt-Fum was grown anaerobically, and cells were then briefly exposed to 100 μM H_2O_2. Catalase was subsequently added to terminate the H_2O_2 stress. Cells were then incubated at 37 °C in the presence of 150 μg/ml chloramphenicol, and fumarase activities were sampled at time points. Data are the average of 3 independent experiments.

the cluster, not the polypeptide.

When H_2O_2 oxidizes the cluster of *E. coli* [4Fe–4S] fumarases, the polypeptide is spared damage as described above [15,19]. However, our inability to reactivate H_2O_2-treated Bt-Fum—in contrast to enzyme oxidized by ferricyanide, O_2^- and O_2—suggested that this rule might not apply to this particular enzyme. Western blots were performed to test if there are carbonylations occurring on Bt-Fum. The results showed

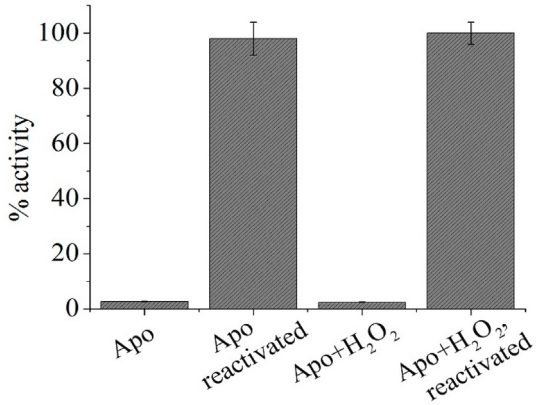

Fig. 4. H_2O_2 does not irreversibly damage the cluster-free Bt-Fum. Purified Bt-Fum in the apoprotein form was reactivated either before or after incubation with 100 μM H_2O_2 for 5 min. Catalase was added to terminate the H_2O_2 stress, and cluster assembly was performed using ferrous iron, DTT, IscS, and cysteine.

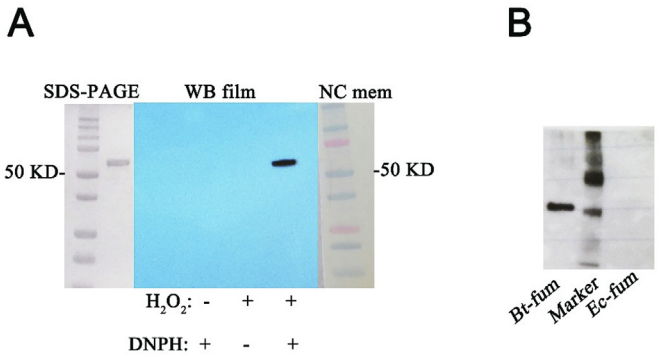

Fig. 5. Bt-Fum but not Ec-Fum is carbonylated upon H_2O_2 treatment. In the anaerobic chamber, 40 nM of anaerobically purified Bt- or Ec-Fum was oxidized by 100 μM H_2O_2 for 5 min. Catalase was added to end the stress, protein carbonyl groups were derivatized with DNPH, and the adducts were visualized by Western blotting. (A) SDS-PAGE analysis of purified Bt-Fum and Western blotting of DNPH-derivatized Bt-Fum. The pre-stained protein ladder transferred to NC membrane is shown at the side of the film to mark the corresponding molecular size. (B) Western blot of H_2O_2-treated and DNPH – derivatized Bt-Fum and Ec-Fum. Only the former enzyme is carbonylated.

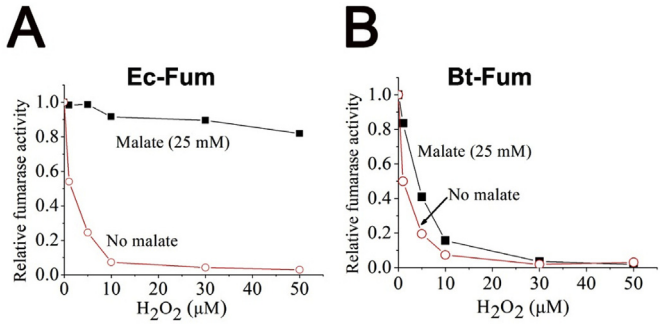

Fig. 6. Substrate protects Ec-Fum but not Bt-Fum against H_2O_2. Purified 10 nM Ec-Fum (Panel A) or Bt-Fum (Panel B) was exposed to 0–50 μM H_2O_2 at room temperature for 8 min. Reactions were performed in anaerobic glove box. Where indicated, 25 mM malate was included in the buffer. Catalase was added after the treatment and residual activity was measured. Measurements were done in duplicate and an average is presented.

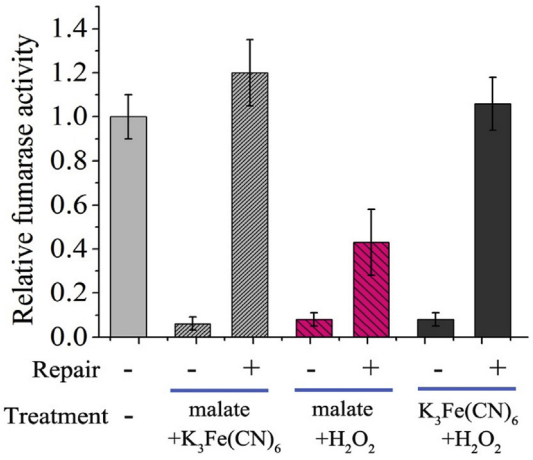

Fig. 7. Malate-saturated Bt-Fum can be damaged by ferricyanide or H_2O_2. A saturating concentration of malate (25 mM) did not block damage to Bt-Fum by 100 μM $K_3Fe(CN)_6$ (gray striped bars) or 100 μM H_2O_2 (red striped bars); the ferricyanide damage was reversible, but the H_2O_2 damage was not. Without malate, 100 μM $K_3Fe(CN)_6$ (5 min) was followed by 100 μM H_2O_2 (black bars); after this treatment the enzyme could be fully reactivated. (For interpretation of the references to color in this figure legend, the reader is referred to the Web version of this article.)

that during H_2O_2 (100 μM) treatment, carbonylated sites were generated on Bt-Fum but not on Ec-Fum(A) (Fig. 5A and B). This outcome suggests that when Bt-Fum was treated by high dose of H_2O_2, a radical species (either $[FeO]^{2+}$ or HO• according to the Fenton reaction) covalently oxidized the polypeptide.

2.4. Substrates cannot protect Bt-Fum against H_2O_2

The solvent – exposed [4Fe–4S] $^{2+}$ cluster of fumarase includes an under-coordinated iron atom that binds substrate. H_2O_2 molecules can penetrate into the active site of these enzymes, bind the critical iron atom, and oxidize the cluster to a redox state that is unstable. Both substrates (malate and fumarate) can protect Ec-Fum when they are added at saturating concentrations [19,32]. Their protective doses correlate with the K_m of the enzyme, indicating that by binding the catalytic iron atom, the substrates block the binding of H_2O_2. However, contrary to the results with Ec-Fum, neither malate and fumarate conferred notable protection on H_2O_2 – treated Bt-Fum (Fig. 6 and Fig. S4), even though the enzyme was fully saturated by high concentrations of substrates (up to 250 mM, which is 30-fold higher than the K_m; Table S1). This result indicated that when the catalytic iron is bound to substrate, H_2O_2 can still oxidize the cluster. Furthermore, H_2O_2 oxidation of malate-saturated Bt-Fum once again generated an enzyme that could only be partially reactivated (Fig. 7). Fenton reactions occur only by inner-sphere electron transfer and therefore require direct iron liganding of H_2O_2. We infer, then, that H_2O_2 attacks at least two sites on the [4Fe–4S] cluster—not only the substrate-binding iron atom, but also another iron atom which potentially has a vacant or weak ligand. Oxidation at this second site led to irreversible protein damage.

Ferricyanide (100 μM) can also inactivate Bt-Fum in the presence of saturating malate, and the treated fumarase can be fully recovered. If substrate was absent and the $K_3Fe(CN)_6$ treatment was followed by 100 μM H_2O_2, Bt-Fum could be completely reactivated—indicating that the irreversible inactivation involves H_2O_2 oxidation of the [4Fe–4S] cluster rather than of a [3Fe–4S] species.

Collectively these data suggest that the Bt-Fum cluster has two sites of potential H_2O_2 access and oxidation, one of which is blocked by substrate and one of which is not. If oxidation occurs at the substrate site, inactivation is reversible; if it occurs at the substrate-independent site, inactivation can be irreversible.

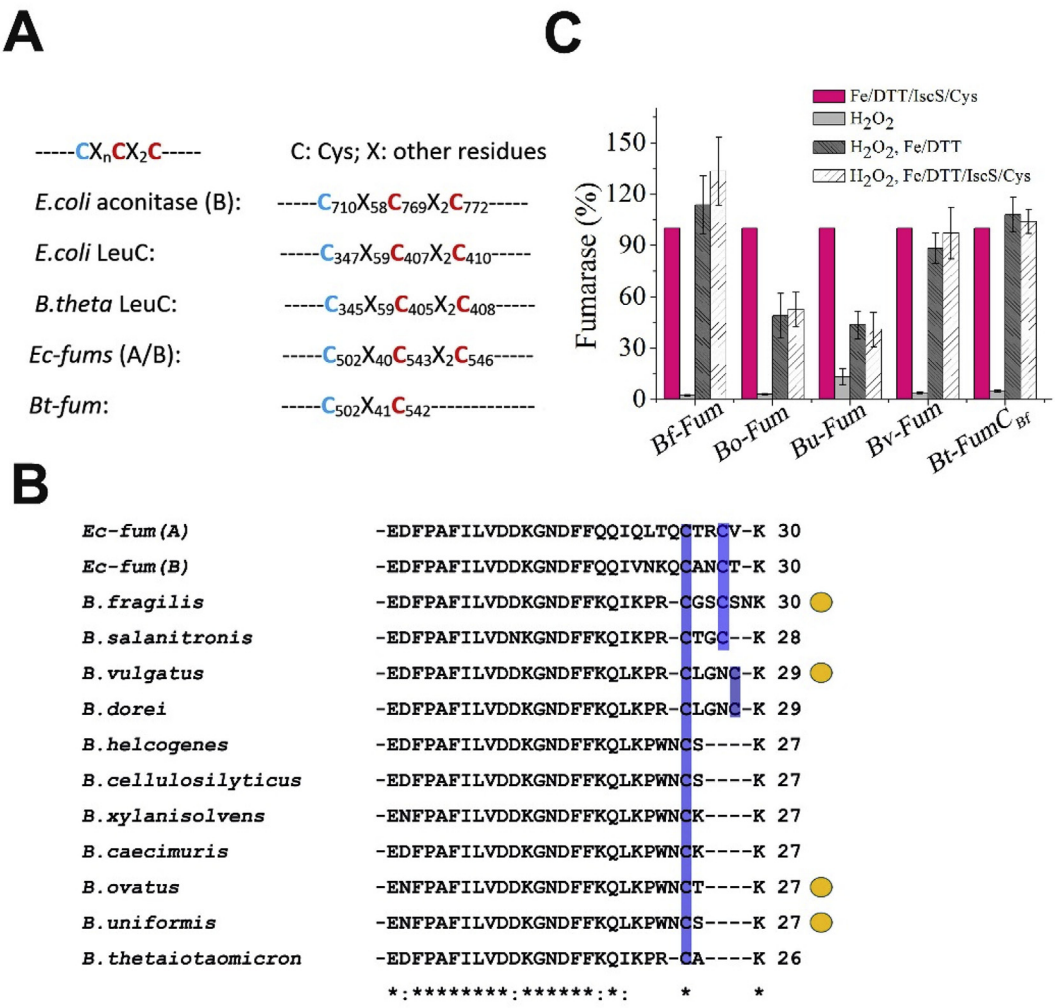

Fig. 8. The lack of a key cysteine at the C-terminus allows H_2O_2 to irreversibly damage fumarases of *Bacteroides*. (A) [4Fe–4S] dehydratases contain a conserved "CX_nCX_2C" motif that coordinates the cluster. (B) C-termini of fumarases from different *Bacteroides species* were aligned by ClustalW 2.0 [56]. Conserved cysteines in the C-terminal "CX_2C" motif were marked in blue. Fumarases of four *Bacteroides species* marked by yellow circles were chosen to be expressed in the *E. coli* and tested for the reversibility of damage upon exposure to H_2O_2. (C) Crude extracts prepared from the SJ54 strain expressing different fumarases were exposed to 100 μM H_2O_2. Enzymes were then repaired by treatment with Fe^{2+}/DTT and/or IscS/Cysteine. Bf-Fum: fumarase of *B. fragilis*; Bo, Bu or Bv-Fum: fumarases of *B. ovatus*, *B. uniformis,* or *B. vulgatus*. Bt-FumC_{Bf}: chimeric Bt-Fum with the C-terminus of *B. fragilis* fumarase. The fumarase activity of each sample is normalized to that of the untreated enzyme. (For interpretation of the references to color in this figure legend, the reader is referred to the Web version of this article.)

2.5. The C-terminus of Bt-Fum lacks the typical motif ligating its [4Fe–4S] cluster

We sought to identify the special feature of Bt-Fum that allows protein-damaging Fenton chemistry to occur, even in substrate-bound form. Surprisingly, we found that, unlike other dehydratases that use three conserved cysteines as ligands for the [4Fe–4S] cluster (**CX_nCX_2C** motif), the sequence of Bt-Fum includes only two cysteines in this motif: a key cysteine is absent at the C-terminus of the protein (Fig. 8A). The C-termini of 7 of 11 fumarases from different *Bacteroides* species lack the C-terminal CX_2C motif (Fig. 8B). To check whether the CX_2C motif is necessary to protect enzymes from irreversible damage, four *Bacteroides* fumarases were expressed in *E.coli* strain SJ54, which lacks both H_2O_2−scavenging ability and endogenous fumarase activity. *B. fragilis* and *B. vulgatus* fumarases have the typical **CX_2C** motifs at their C-termini, and after treatment by 100 μM H_2O_2 their activity could be completely restored. In contrast, *B. ovatus* and *B. uniformis* fumarases lack the motif, and their H_2O_2−destroyed activities were only partially (30%–55%) restored (Fig. 8C).

To further test whether the absence of the C-terminal CX_2C motif is responsible for the irreversible damage to Bt-Fum, we attempted to construct a chimeric protein containing the C-terminal CX_2C motif of Ec-Fum. In a set of constructions C-terminus of Bt-Fum was replaced with that of Ec-Fum(A) (ranging from 4 to 10 residues). However, none of these constructions showed activity (data not shown), probably because the local structure at the C-terminus was disrupted due to incompatibilities of the two enzymes. Since *B. fragilis* is evolutionarily closer to *B. thetaiotaomicron*, the C-terminal 6 residues "GSCSNK" of *B. fragilis* fumarase were then used to replace the terminal AK residues of Bt-Fum. The ensuing chimeric fumarase (denoted Bt-FumC_{Bf}) was active (Fig. 8C). Strikingly, it lost activity upon 100 μM H_2O_2 treatment (5 min), but full activity was regained when the cluster was repaired (Fig. 8C).

These results supported the hypothesis: the absence of the C-terminal CX_2C motif makes the [4Fe–4S] cluster more labile in fumarases and prone to be damaged by high levels of H_2O_2, resulting in the production of strong radical species and subsequent polypeptide oxidation. We infer that the radical species causing irreversible damage may originate from oxidation of a second cluster iron atom that is ligated by nothing or by a non-cysteinyl residue (Fig. 9). Low doses of H_2O_2 did not generated irreversible damage (Fig. S3), indicating that the second ROS-targeting iron might be weakly liganded, thus somewhat

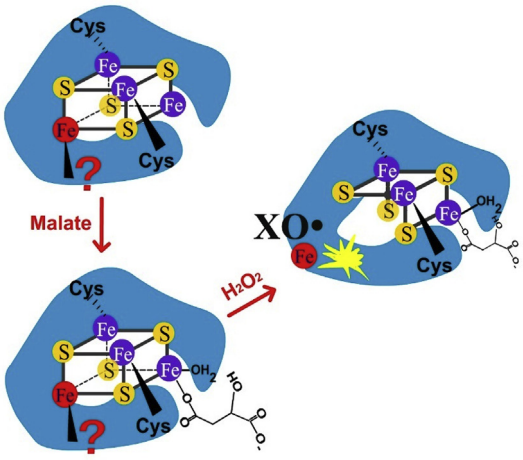

Fig. 9. Model of Bt-Fum oxidation by high dose of H_2O_2. Substrate binds at the catalytic iron atom (blue violet). A second cluster iron atom (red) lacks a cysteine ligand and can still be oxidized by H_2O_2. This oxidation generates a hydroxyl-like radical species (XO•, X: Fe or H) that frequently oxidizes the polypeptide, precluding repair in vitro or in vivo. (For interpretation of the references to color in this figure legend, the reader is referred to the Web version of this article.)

diminishing the rate of its reaction with H_2O_2.

A phylogenetic tree constructed from a multiple sequence alignment of *Bacteroides* fumarase sequences shows a different pattern of relatedness with respect to the C-termini (Fig. 10). The fumarases without the C-terminal **C**X_2**C** motifs, such as those from *B. thetaiotaomicron* and *B. ovatus*, form their own distinct clade, as do those fumarases with **C**X_2**C** motifs, including those of *B. fragilis* and *B. salanitronis*. This result suggested that even though these bacteria all belong to *Bacteroides* sp., they evolved [4Fe–4S] fumarases with distinct coordination of their clusters.

3. Discussion

The consensus obtained from previous studies is that when H_2O_2 oxidizes iron-sulfur clusters, H_2O_2 picks up two consecutive electrons from the cluster, the $[FeO]^{2+}$ does not covalently oxidize the peptide, and the reaction releases an innocuous hydroxide anion instead of HO•. Therefore, oxidative inactivation is reversible, and cells can rapidly recover from stress. In this study, it has been proved that, with higher doses of H_2O_2, the fumarases from anaerobic *Bacteroides* species suffer carbonylation of their polypeptide chains. These irreversible damages were not observed upon treatments with non-H_2O_2 oxidants, such as $K_3Fe(CN)_6$, O_2^- and molecular O_2. H_2O_2 cannot directly oxidize the polypeptide of apo-protein, indicating that the oxidation is catalyzed by the cluster. Thus, the radical species that is formed during the H_2O_2 oxidation attacks the fumarases of these strict anaerobes. It is unclear whether the damaging radical species is $[FeO]^{2+}$ or HO•. In any case, it seems apparent that the ferryl radical formed in Bt-Fum fails to pull a second electron from the cluster itself. Bt-Fum lacks a key cysteine residue that the [4Fe–4S] cluster, and it seems likely that another residue has substituted for the missing cysteine ligand. If so, the redox potential of the cluster might vary from those with cysteine-only ligands. Iron-sulfur clusters with histidine ligands have a higher reduction potential than clusters ligated only by cysteines [33]. Perhaps $[FeO]^{2+}$ that is formed during the H_2O_2 oxidation of Bt-Fum is slow to pull another electron from the cluster, due to the increased potential. Alternatively, the ferryl-bound cluster may abstract an electron from the novel ligand, rather than from a cysteine ligand, generating a carbonyl moiety and eradicating any possibility of reforming the cluster.

Interestingly, analogous events occur when H_2O_2 oxidizes the ferrous iron atoms of mononuclear enzymes. If the iron binding site includes a cysteine ligand, the nascent hydroxyl-like radical immediately oxidizes it, forming cysteine sulfenic acid or a disulfide bond. The enzyme can subsequently be reactivated by reduction of the oxidized cysteine and re-binding of ferrous iron. However, if the iron atom lacks any cysteine ligand, the radical oxidizes the polypeptide and inactivation is irreversible [31,34].

Under the conditions of our experiments, low doses of H_2O_2 predominantly left the enzyme in a reactivatable [3Fe–4S] form. This event circumvented second-site oxidation. However, it is worth noting that in vivo this species would be quickly repaired, allowing further cycles of oxidation—potentially until the majority of enzyme had suffered irreversible second-site damage. This possibility is sharpened by the fact that as a pathway bottleneck develops, the substrate of the vulnerable enzyme accumulates, thereby blocking oxidation of the catalytic iron atom and allowing irreversible oxidation of the secondary iron atom. Long-term experiments will be necessary to test this possibility.

Fumarase is conserved in organisms from bacteria to eukaryotes. They have been classified in two groups, depending upon whether they employ clusters for catalysis. Class I, exclusively found in bacteria, contain an ROS-sensitive catalytic [4Fe–4S] cluster. The class II fumarases, such as the *E. coli* FumC and eukaryotic fumarases, are iron-independent and therefore oxidant-resistant [35,36]. Our data present

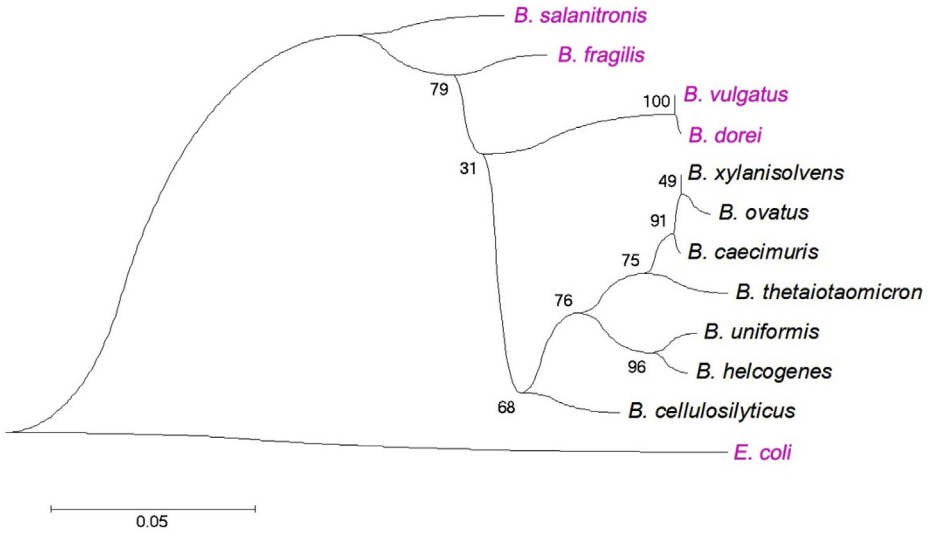

Fig. 10. Phylogenetic tree of fumarases amino acid sequences from *Bacteroides* species. Sequences were aligned with the ClustalW 2.0 program [56]. The tree was obtained with the Maximum Likelihood analysis. Bootstrapping analyses (1000 bootstrap replicates) have been tested on the Maximum Likelihood methods to examine the confidence of nodes. Fumarases with the C-terminal "CX_2C" motif are shown in red. The scale bar indicates 0.05 amino acid change expected per site. (For interpretation of the references to color in this figure legend, the reader is referred to the Web version of this article.)

the possibility that the protein became progressively resistant to oxidants over the course of evolution. The most abundant human intestinal anaerobes such as *B. thetaiotaomicron*, which may have evolved from the sediment-dwelling ancient microbes that arose in an anaerobic world during the early evolutionary process, utilize a single fumarase (class I) with an oxidatively labile [4Fe–4S] cluster as prosthetic group; the facultative anaerobe *E. coli*, which enjoys both anaerobic and aerobic lifestyles, expresses three fumarases, one of which is cluster-independent class II (Fum C). Because Fum C is resistant to ROS, it is induced when *E. coli* senses oxidative stress through its transcription factor SoxR. Strikingly, aerobic eukaryotes have fully abandoned the oxygen − unstable class I fumarases, exclusively using homologues of FumC [36,37]. Since fumarase is a key enzyme involved in cellular central metabolism, the benefits organisms can receive through adopting oxygen-resistant fumarase are obvious.

As demonstrated in this study, bacteria have also made subtle structural modifications on the cluster-containing fumarases that affect their tolerance of H_2O_2 stress. Full coordination of the cluster by the conserved motif (**CX_nCX_2C**) evidently avoids covalent enzyme modification and thereby allows the enzyme to be repaired in H_2O_2 − stressed cells. Repair processes occur within minutes, and so during H_2O_2 stress the steady-state activity of the enzyme—and thus its ability to sustain flux through the TCA cycle—depends upon the balance between damage and repair. Analysis of a phylogenetic tree constructed from a multiple sequence alignment of *Bacteroides* fumarases showed that these enzymes are distinctly clustered in separate branches; *B. fragilis* fumarase is a representative in one group and Bt-Fum is on behalf of another. *B. fragilis* and *B. thetaiotaomicron* belong to a very close and distinct phylum based on their 16S rRNA homology sequences. *B. fragilis* shares 21–36% DNA identity with *B. thetaiotaomicron* [38]. Both organisms have been the subjects of studies of oxidative stress, which raises the prospect that insight may be derived by looking at their different tolerance to it.

These bacteria are both opportunistic pathogens, but *B. fragilis* is more likely to be isolated from intra-abdominal abscesses [22,39]. It has been shown that its resistance to oxidative stress is important for establishment of intra-abdominal abscesses, as oxidative stress occurs immediately when *B. fragilis* translocates from the anaerobic intestine to the more oxygenated (6% O_2) peritoneal cavity [40,41]. Furthermore, more-severe oxidative stress resulting from the immune response requires that *B. fragilis* express its OxyR response to H_2O_2 during abscess formation [39,42]. Indeed, other observations also suggest that *B. fragilis* has evolved to be more oxygen-resistant than is *B. thetaiotaomicron*. *B. fragilis* has been shown to exploit the presence of low levels of oxygen through its cytochrome bd-oxidase-dependent respiratory chain [42]. It also features both oxygen-sensitive and oxygen-dependent ribonucleotide reductases, indicating that in its native lifestyle it sometimes replicates its DNA in oxygen-containing environments. In contrast, *B. thetaiotaomicron* only has the anaerobic-style oxygen-sensitive isozyme [20,43]. In this context, it may be important that *B. fragilis* features a fumarase that is relatively H_2O_2-resistant, whereas the *B. thetaiotaomicron* enzyme is more vulnerable.

Obligate anaerobes such as *Bacteroides* are the most abundant members within human gut microbiota. In this environment oxygen levels fall rapidly between the oxic epithelial surface and the anoxic lumen [44]. There is compelling circumstantial evidence that H_2O_2 may arise in this habitat. *Bacteroides* species have robust OxyR and PerR systems that have evolved to defend these bacteria against H_2O_2 [45–47], and the co-resident *E. coli* feature a cytochrome c peroxidase that is induced when H_2O_2 is present but oxygen is absent [48,49]. The source of the putative H_2O_2 is unclear, but it might plausibly be generated by chemical reactions at the oxic/anoxic interface, by lactic acid bacteria that live there, or by the host immune response during episodes of inflammation. The oxidative stress may become especially acute when the O_2 availability in colon increases during antibiotic treatment or pathogen expansion [50,51]. Since fumarase is essential for the core metabolism of *Bacteroides* species, its inactivation during periods of H_2O_2 stress might impair its growth and contribute to gut dysbiosis.

Moving forward, it will be of interest to determine how the cluster of Bt-Fum is coordinated. Although the [4Fe–4S] clusters are usually bound to the polypeptide by cysteinyl residues, other residues like histidine, glutamine and aspartic acid can also function as atypical ligands in rare cases. For example, in the nitric oxide sensor (NsrR) from *Streptomyces coelicolor,* Asp is the fourth ligand to the [4Fe–4S] cluster further coordinated by three invariant Cys residues; the [NiFe] hydrogenase from strict anaerobe *Desulfovibrio gigas* have a ligand from a histidinyl residue [6,52,53]. Metabolites can also stabilize clusters, such as the thiolate donating ligand like glutathione [33]. Our data imply that the site which is not liganded by cysteine in the cluster of Bt-Fum is either open or breathable, enabling H_2O_2 access to the cluster.

The idea that evolution has tinkered with fumarase to adjust its sensitivity to oxidants conforms with similar observations of other ROS-sensitive enzyme classes. Chloroplasts, which are sites of photosynthetic ROS formation, cofactor their IPMI enzymes with stable [2Fe–2S] clusters rather than the unstable [4Fe–4S] variety [54]. The other primary target of H_2O_2 inside cells are mononuclear enzymes that employ a single divalent transition metal to catalyze non-redox reactions. In *E. coli* these enzymes routinely use ferrous iron as the catalytic metal—but they shift to manganese, which does not react with H_2O_2, when the OxyR system detects rising levels of H_2O_2 stress [55]. In Mycobacteria, which reside in granulomas that are exposed to the oxidative bursts of neutrophils, ferrous iron is replaced by a ferric complex, and it is suspected that they are cofactored by manganese in H_2O_2-forming lactic acid bacteria [55]. Other examples of enzymes that have evolved towards oxidant tolerance include hydrogenases and, to some extent, nitrogenases and glycyl-radical enzymes. In all the cases, most of the structural features of the ancestral, oxidant-sensitive enzymes have been retained; instead, regions near the vulnerable cofactors have been tweaked. Thus the contrast between the subfamilies of *Bacteroides* fumarases may been part of this broad pattern of retrofitting.

4. Materials and methods

4.1. Chemicals

Brain heart infusion (BHI) broth, haemin, L-cysteine, L-cystine, fumaric acid, $Fe(NH_4)_2(SO_4)_2$, dithiothreitol, maltose, β-lactose, 2,2′-dipyridyl, citraconate, disodium L-malic acid, DL-trisodium isocitrate, xanthine and xanthine oxidase from bovine milk, catalase, *E. coli* iron-containing SOD, IPTG, imidazole, were bought from Sigma, D-glucose was obtained from Fisher Scientific, His Gravitrap, from GE Healthcare. Antibiotics (ampicillin and chloramphenicol) were all Sigma products.

4.2. Cell growth and media

Anaerobic cultures were grown at 37 °C in an anaerobic glove box (Coy Laboratory Products) containing 85% N_2, 10% H_2 and 5% CO_2, BHIS medium for *B. thetaiotaomicron*, LB and minimal A media for *E. coli* were made as previous literatures. Media for anaerobic cultures were prepared by autoclaving and kept in anaerobic chamber to be degassed for at least 24 h before use. Strains and plasmids are listed in Table S2.

4.3. Expression of fumarases in SJ54 strain

To express Ec-Fum(A) in *E. coli* strain of *fumABC* and catalase/peroxidase mutants (SJ54), encoding genes were cloned behind the *lac* promoter of pWKS30 vector by *Hin*dIII/*Bam*HI. To express the fumarase of *B. fragilis*, *B. vulgatus, B. ovatus* and *B. uniformis,* the genomic DNA was extracted by genomic DNA extraction kit (Qiagen) from the *Bacteroides* cells grown in anaerobic BHIS media, PCR was conducted

using respective primers, DNA was digested by *Sac*I/*Xba*I and inserted into the vector pCKR101. For the expressions, RBS of *E. coli gapA* was inserted upstream of the gene. Construction was confirmed by digestion. The plasmid was then anaerobically transformed into SJ54 competent cells prepared by $CaCl_2$ method, transformants were screened on LB plates (100 μg/ml ampicillin). Sequences of primers for PCR are listed in Table S3. To induce the expression in SJ54, minimal A media was used, 0.2% lactose was added as the inducer.

4.4. Enzyme assays

To measure the activity of cluster-containing enzymes in cell extracts, cells were harvested and resuspended in anaerobic buffers, cell extracts were prepared by sonication in an anaerobic chamber. Reactions were prepared anaerobically using sealable cuvettes, and then moved outside of the anaerobic chamber to monitor activities. The fumarase activity was determined in 50 mM sodium phosphate (pH 7.3) containing 50 mM of L-malate; production of fumarate was monitored at 250 nm. K_m values were measured with different concentrations of substrates as substrate; the value was calculated from a Lineweaver-Burk plot. IPMI activity was measured by monitoring the absorbance's decrease of citraconate at 235 nm in 100 mM Tris-Cl (pH 7.6). Protein concentrations were determined using the Coomassie protein assay reagent (Pierce) with BSA as the standard.

4.5. In vitro inactivation and repair of fumarase and IPMI

For the in vitro inactivation of H_2O_2, 50 μM or 100 μM H_2O_2 was added to 100 μl NaPi buffer (pH 7.2) containing cell extracts or purified fumarase, reactions were kept at room temperature for specific time in anaerobic chamber; enzymes activities were measured in sealed cuvettes, as described above.

To use $K_3Fe(CN)_6$ to damage fumarase, in 100 μl anaerobic NaPi buffer (pH 7.2), 100 μM $K_3Fe(CN)_6$ was added to anaerobically prepared cell debris, reaction was kept in anaerobic chamber at room temperature for 10 min.

For the inactivation of O_2^- on fumarase, xanthine and xanthine oxidase were quickly added to anaerobically prepared cell extracts to generate O_2^- in the presence of O_2 and inactivate fumarase at room temperature, in the reaction, O_2^- was produced at a rate about 0.9 μM/min. Catalase (200 U/ml) was included in the assay to degrade the potentially produced H_2O_2. After 6 min, the loss of fumarase activity was monitored at 250 nm.

To inactivate fumarase by molecular O_2, purified and reactivated Bt-Fum was exposed to air at room temperature, saturated concentration of O_2 (~210 μM) was introduced by pipetting the solution along the cuvette wall at intervals. Excess catalase and SOD (both were 500 U/ml) were always included in the assays, reaction was kept for 1 h, till fumarase activity was measured.

For repairing the fumarase damaged by $K_3Fe(CN)_6$, O_2^-, or molecular O_2, the anaerobic reactivating system contained 1 mM Fe $(NH_4)_2(SO_4)_2$, 2.5 mM DTT, the reaction was anaerobically incubated for 35 min at room temperature; for reactivating H_2O_2−treated fumarase, 2.8 mM cysteine and 0.15 μM purified *E. coli* IscS protein were further supplemented into the above repairing system, reaction was anaerobically incubated for 1–2 h at room temperature.

4.6. In vivo repair of fumarase inactivated by H_2O_2

SJ54 cells expressing Ec-Fum or Bt-Fum was grown anaerobically, cells were incubated for 8 min with 100 μM exogenous H_2O_2, H_2O_2 can penetrate into cells. Catalase was subsequently added to terminate H_2O_2 stress. To block further protein synthesis, 150 μg/ml chloramphenicol was supplemented, cells were then kept at 37 °C, cell extracts were prepared over time and fumarase activity was measured.

4.7. EPR analysis

Purified Ec-Fum(A) or Bt-Fum was repaired for the cluster assembly in the absence of O_2, as described above, solutions were triply filtered by centrifugal tubes (Millipore), to get rid of extra Fe^{2+} and DTT, fumarase activity was measured to confirm the cluster has been successfully rebuilt, then the sample was incubated with H_2O_2 for specific time and activity was detected again to prove the inactivation. Samples were then transferred into an EPR tube and frozen in dry ice. EPR spectra of [3Fe–4S] clusters were measured at the following settings: microwave power, 1 mW; microwave frequency, 9.05 GHz; modulation amplitude, 8 G at 100 KHz; and time constant, 0.032.

4.8. Protein carbonylation

200 ml Bl21 (DE3) harboring the expression plasmid pET 16b-Bt-Fum or pET 16b-Ec-Fum (A) anaerobic culture was prepared to over express of Bt-Fum or Ec-Fum (A) by pET 16 vector, protein purification by NTA resins was performed. Same amount (40 nM) of reactivated protein was then oxidized by 100 μM H_2O_2 for 5 min, catalase was added to eliminate the stress, protein carbonyl groups were derivatized with DNPH. All purification and inactivation steps were conducted anaerobically at chamber temperature (27 °C), all buffers were anaerobic. The adducts after derivatization were moved out of the chamber and visualized by Western blotting.

4.9. Construction of chimeric fumarase

To construct Bt-Fum with C-terminal 6 residues “GSCSNK” of *B. fragilis* fumarase replacing its C-terminal 2 residues “AK”, the open reading frames of *B. fragilis* fumarase-encoding gene was PCR amplified from *B. fragilis* by using the primers in Table S3, the DNA sequence encoding 6 residues “GSCSNK” was added to the reverse primer upstream of the stop codon. The PCR product were digested with *Sac*I and *Xba*I and cloned into pCKR101 vector. The plasmid constructions were confirmed by restriction/sequencing analyses. The protein was expressed in glucose/0.4 mM IPTG media.

4.10. Phylogenetic analyses

Homologues of Bt-Fum in *Bacteroides* species were first retrieved at the NCBI database using the *TBLASTn* program, amino acid sequences were aligned using ClustalW 2.0 program [56], Phylogenetic tree was calculated using MEGA 5 [57] by the Maximum Likelihood method. The confidence limits were estimated by using 1000 bootstrapping replicates.

Conflicts of interest

The authors declare no conflict of interest.

Acknowledgements

We thank Dr. Mark Nilges of the Illinois EPR Research Center for assistance with EPR experiments, and we thank Dr. Degnan Patrick and Dr. Yuanyuan Liu for providing *Bacteroides* strains. This work was supported by the National Natural Science Foundation of China (No. 31970101), the Research Start-up Funding of Shantou University (NTF18018) and Grant (GM049640) from National Institutes of Health (NIH).

Appendix A. Supplementary data

Supplementary data to this article can be found online at https://doi.org/10.1016/j.redox.2019.101296.

References

[1] H. Beinert, R.H. Holm, E. Munck, Iron-sulfur clusters: nature's modular, multipurpose structures, Science 277 (1997) 653–659, https://doi.org/10.1126/science.277.5326.653.

[2] D.C. Johnson, D.R. Dean, A.D. Smith, M.K. Johnson, Structure, function, and formation of biological iron-sulfur clusters, Annu. Rev. Biochem. 74 (2005) 247–281, https://doi.org/10.1146/annurev.biochem.74.082803.133518.

[3] E.L. Mettert, P.J. Kiley, Fe-S proteins that regulate gene expression, Biochim. Biophys. Acta Mol. Cell Res. 1853 (2015) 1284–1293, https://doi.org/10.1016/j.bbamcr.2014.11.018.

[4] G.Q. Tan, J.X. Lu, J.P. Bitoun, H. Huang, H.G. Ding, IscA/SufA paralogues are required for the [4Fe-4S] cluster assembly in enzymes of multiple physiological pathways in Escherichia coli under aerobic growth conditions, Biochem. J. 420 (2009) 463–472, https://doi.org/10.1042/Bj20090206.

[5] L. Banci, F. Camponeschi, S. Ciofi-Baffoni, M. Piccioli, The NMR contribution to protein-protein networking in Fe-S protein maturation, J. Biol. Inorg. Chem. 23 (2018) 665–685, https://doi.org/10.1007/s00775-018-1573-5.

[6] H. Beinert, Iron-sulfur proteins: ancient structures, still full of surprises, J. Biol. Inorg. Chem. 5 (2000) 2–15.

[7] B. Py, F. Barras, Building Fe-S proteins: bacterial strategies, Nat. Rev. Microbiol. 8 (2010) 436–446, https://doi.org/10.1038/nrmicro2356.

[8] S. Todorovic, M. Teixeira, Resonance Raman spectroscopy of Fe-S proteins and their redox properties, J. Biol. Inorg. Chem. 23 (2018) 647–661, https://doi.org/10.1007/s00775-018-1533-0.

[9] J.A. Imlay, The molecular mechanisms and physiological consequences of oxidative stress: lessons from a model bacterium, Nat. Rev. Microbiol. 11 (2013) 443–454, https://doi.org/10.1038/nrmicro3032.

[10] A. Ligeza, A.N. Tikhonov, J.S. Hyde, W.K. Subczynski, Oxygen permeability of thylakoid membranes: electron paramagnetic resonance spin labeling study, Biochim. Biophys. Acta 1365 (1998) 453–463.

[11] Z. Lu, J.A. Imlay, The fumarate reductase of Bacteroides thetaiotaomicron, unlike that of Escherichia coli, is configured so that it does not generate reactive oxygen species, mBio 8 (2017), https://doi.org/10.1128/mBio.01873-16 e01873-01816.

[12] D.H. Flint, R.M. Allen, Iron-sulfur proteins with nonredox functions, Chem. Rev. 96 (1996) 2315–2334.

[13] P.R. Gardner, I. Fridovich, Superoxide sensitivity of the Escherichia coli 6-phosphogluconate dehydratase, J. Biol. Chem. 266 (1991) 1478–1483.

[14] S.I. Liochev, I. Fridovich, Fumarase C, the stable fumarase of Escherichia coli, is controlled by the soxRS regulon, Proc. Natl. Acad. Sci. U. S. A. 89 (1992) 5892–5896.

[15] L. Macomber, J.A. Imlay, The iron-sulfur clusters of dehydratases are primary intracellular targets of copper toxicity, Proc. Natl. Acad. Sci. U. S. A. 106 (2009) 8344–8349, https://doi.org/10.1073/pnas.0812808106.

[16] B. Roche, L. Aussel, B. Ezraty, P. Mandin, B. Py, F. Barras, Iron/sulfur proteins biogenesis in prokaryotes: formation, regulation and diversity, Biochim. Biophys. Acta 1827 (2013) 455–469, https://doi.org/10.1016/j.bbabio.2012.12.010.

[17] B. Halliwell, J.M. Gutteridge, Role of free radicals and catalytic metal ions in human disease: an overview, Methods Enzymol. 186 (1990) 1–85.

[18] S. Varghese, Y. Tang, J.A. Imlay, Contrasting sensitivities of Escherichia coli aconitases A and B to oxidation and iron depletion, J. Bacteriol. 185 (2003) 221–230, https://doi.org/10.1128/jb.185.1.221-230.2003.

[19] S. Jang, J.A. Imlay, Micromolar intracellular hydrogen peroxide disrupts metabolism by damaging iron-sulfur enzymes, J. Biol. Chem. 282 (2007) 929–937, https://doi.org/10.1074/jbc.M607646200.

[20] M.K. Bacic, C.J. Smith, Laboratory maintenance and cultivation of bacteroides species, Curr Protoc Microbiol (2008), https://doi.org/10.1002/9780471729259.mc13c01s9 (Chapter 13): 13C.1.1-13C.1.21.

[21] A.A. Salyers, Bacteroides of the human lower intestinal tract, Annu. Rev. Microbiol. 38 (1984) 293–313, https://doi.org/10.1146/annurev.mi.38.100184.001453.

[22] H.M. Wexler, *Bacteroides*: the good, the bad, and the nitty-gritty, Clin. Microbiol. Rev. 20 (2007) 593–621, https://doi.org/10.1128/CMR.00008-07.

[23] Z. Lu, R. Sethu, J.A. Imlay, Endogenous superoxide is a key effector of the oxygen sensitivity of a model obligate anaerobe, Proc. Natl. Acad. Sci. U. S. A. 115 (2018) E3266–E3275, https://doi.org/10.1073/pnas.1800120115.

[24] N. Pan, J.A. Imlay, How does oxygen inhibit central metabolism in the obligate anaerobe Bacteroides thetaiotaomicron, Mol. Microbiol. 39 (2001) 1562–1571, https://doi.org/10.1046/j.1365-2958.2001.02343.x.

[25] L.C. Seaver, J.A. Imlay, Hydrogen peroxide fluxes and compartmentalization inside growing Escherichia coli, J. Bacteriol. 183 (2001) 7182–7189, https://doi.org/10.1128/JB.183.24.7182-7189.2001.

[26] J.P. Bitoun, G.F. Wu, H.G. Ding, Escherichia coli FtnA acts as an iron buffer for re-assembly of iron-sulfur clusters in response to hydrogen peroxide stress, Biometals 21 (2008) 693–703, https://doi.org/10.1007/s10534-008-9154-7.

[27] X. Li, J.A. Imlay, Improved measurements of scant hydrogen peroxide enable experiments that define its threshold of toxicity for Escherichia coli, Free Radic. Biol. Med. 120 (2018) 217–227, https://doi.org/10.1016/j.freeradbiomed.2018.03.025.

[28] O. Djaman, F.W. Outten, J.A. Imlay, Repair of oxidized iron-sulfur clusters in Escherichia coli, J. Biol. Chem. 279 (2004) 44590–44599, https://doi.org/10.1074/jbc.M406487200.

[29] S.A. Freibert, B.D. Weiler, E. Bill, A.J. Pierik, U. Muhlenhoff, R. Lill, Biochemical reconstitution and spectroscopic analysis of iron-sulfur proteins, Methods Enzymol. 599 (2018) 197–226, https://doi.org/10.1016/bs.mie.2017.11.034.

[30] A. Marquet, B.T.S. Bui, A.G. Smith, M.J. Warren, Iron-sulfur proteins as initiators of radical chemistry, Nat. Prod. Rep. 24 (2007) 1027–1040, https://doi.org/10.1039/b703109m.

[31] A. Anjem, J.A. Imlay, Mononuclear iron enzymes are primary targets of hydrogen peroxide stress, J. Biol. Chem. 287 (2012) 15544–15556, https://doi.org/10.1074/jbc.M111.330365.

[32] S. Jang, J.A. Imlay, Hydrogen peroxide inactivates the Escherichia coli Isc iron-sulphur assembly system, and OxyR induces the Suf system to compensate, Mol. Microbiol. 78 (2010) 1448–1467, https://doi.org/10.1111/j.1365-2958.2010.07418.x.

[33] D.W. Bak, S.J. Elliott, Alternative FeS cluster ligands: tuning redox potentials and chemistry, Curr. Opin. Chem. Biol. 19 (2014) 50–58, https://doi.org/10.1016/j.cbpa.2013.12.015.

[34] J.W. Lee, J.D. Helmann, The PerR transcription factor senses H2O2 by metal-catalyzed histidine oxidation, Nature 440 (2006) 363–367, https://doi.org/10.1038/nature04537.

[35] Y. Ueda, N. Yumoto, M. Tokushige, K. Fukui, H. Ohya-Nishiguchi, Purification and characterization of two types of fumarase from Escherichia coli, J. Biochem. 109 (1991) 728–733, https://doi.org/10.1093/oxfordjournals.jbchem.a123448.

[36] S.A. Woods, S.D. Schwartzbach, J.R. Guest, Two biochemically distinct classes of fumarase in Escherichia coli, Biochim. Biophys. Acta 954 (1988) 14–26.

[37] R.A. Alberty, Fumarase, the Enzymes vols. 531–544, Academic Press, New York, 1959.

[38] E.R. Rocha, C.J. Smith, Ferritin-like family proteins in the anaerobe Bacteroides fragilis: when an oxygen storm is coming, take your iron to the shelter, Biometals 26 (2013) 577–591, https://doi.org/10.1007/s10534-013-9650-2.

[39] C.J. Sund, E.R. Rocha, A.O. Tzianabos, W.G. Wells, J.M. Gee, M.A. Reott, D.P. O'Rourke, C.J. Smith, The Bacteroides fragilis transcriptome response to oxygen and H(2)O(2): the role of OxyR and its effect on survival and virulence, Mol. Microbiol. 67 (2008) 129–142, https://doi.org/10.1111/j.1365-2958.2008.06269.x.

[40] M.I. Betteken, E.R. Rocha, C.J. Smith, Dps and DpsL mediate survival in vitro and in vivo during the prolonged oxidative stress response in Bacteroides fragilis, J. Bacteriol. 197 (2015) 3329–3338, https://doi.org/10.1128/JB.00342-15.

[41] Y.L. Cao, E.R. Rocha, C.J. Smith, Efficient utilization of complex N-linked glycans is a selective advantage for Bacteroides fragilis in extraintestinal infections, Proc. Natl. Acad. Sci. U. S. A. 111 (2014) 12901–12906, https://doi.org/10.1073/pnas.1407344111.

[42] A.D. Baughn, M.H. Malamy, The strict anaerobe Bacteroides fragilis grows in and benefits from nanomolar concentrations of oxygen, Nature 427 (2004) 441–444, https://doi.org/10.1038/nature02285.

[43] D. Smalley, E.R. Rocha, C.J. Smith, Aerobic-type ribonucleotide reductase in the anaerobe Bacteroides fragilis, J. Bacteriol. 184 (2002) 895–903, https://doi.org/10.1128/jb.184.4.895-903.2002.

[44] M.G. Espey, Role of oxygen gradients in shaping redox relationships between the human intestine and its microbiota, Free Radic. Biol. Med. 55 (2013) 130–140, https://doi.org/10.1016/j.freeradbiomed.2012.10.554.

[45] E.R. Rocha, C.D. Herren, D.J. Smalley, C.J. Smith, The complex oxidative stress response of Bacteroides fragilis: the role of OxyR in control of gene expression, Anaerobe 9 (2003) 165–173, https://doi.org/10.1016/S1075-9964(03)00118-5.

[46] K.R. Strand, C. Sun, F.E. Jenney Jr., G.J. Schut, M.W. Adams, Oxidative stress protection and the repair response to hydrogen peroxide in the hyperthermophilic archaeon Pyrococcus furiosus and in related species, Arch. Microbiol. 192 (2010) 447–459, https://doi.org/10.1007/s00203-010-0570-z.

[47] S. Mishra, J.A. Imlay, An anaerobic bacterium, Bacteroides thetaiotaomicron, uses a consortium of enzymes to scavenge hydrogen peroxide, Mol. Microbiol. 90 (2013) 1356–1371, https://doi.org/10.1111/mmi.12438.

[48] J.D. Partridge, R.K. Poole, J. Green, The Escherichia coli yhjA gene, encoding a predicted cytochrome c peroxidase, is regulated by FNR and OxyR, Microbiology 153 (2007) 1499–1507, https://doi.org/10.1099/mic.0.2006/004838-0.

[49] M. Khademian, J.A. Imlay, Escherichia coli cytochrome c peroxidase is a respiratory oxidase that enables the use of hydrogen peroxide as a terminal electron acceptor, Proc. Natl. Acad. Sci. U.S.A. 114 (2017) E6922–E6931, https://doi.org/10.1073/pnas.1701587114.

[50] L. Rigottier-Gois, Dysbiosis in inflammatory bowel diseases: the oxygen hypothesis, ISME J. 7 (2013) 1256–1261, https://doi.org/10.1038/ismej.2013.80.

[51] F. Rivera-Chavez, C.A. Lopez, A.J. Baumler, Oxygen as a driver of gut dysbiosis, Free Radic. Biol. Med. 105 (2017) 93–101, https://doi.org/10.1016/j.freeradbiomed.2016.09.022.

[52] A. Volbeda, M.H. Charon, C. Piras, E.C. Hatchikian, M. Frey, J.C. Fontecilla-Camps, Crystal structure of the nickel-iron hydrogenase from Desulfovibrio gigas, Nature 373 (1995) 580–587, https://doi.org/10.1038/373580a0.

[53] A. Volbeda, E.L. Dodd, C. Darnault, J.C. Crack, O. Renoux, M.I. Hutchings, N.E. Le Brun, J.C. Fontecilla-Camps, Crystal structures of the NO sensor NsrR reveal how its iron-sulfur cluster modulates DNA binding, Nat. Commun. 8 (2017) Artn 1505210.1038/Ncomms15052.

[54] J.A. Imlay, R. Sethu, S.K. Rohaun, Evolutionary adaptations that enable enzymes to tolerate oxidative stress, Free Radic. Biol. Med. (2019), https://doi.org/10.1016/j.freeradbiomed.2019.01.048 [Epub ahead of print].

[55] J.A. Imlay, Where in the world do bacteria experience oxidative stress? Environ. Microbiol. 21 (2018) 521–530, https://doi.org/10.1111/1462-2920.14445.

[56] J.D. Thompson, D.G. Higgins, T.J. Gibson, Clustal W: improving the sensitivity of progressive multiple sequence alignment through sequence weighting, position-specific gap penalties and weight matrix choice, Nucleic Acids Res. 22 (1994) 4673–4680, https://doi.org/10.1093/nar/22.22.4673.

[57] K. Tamura, D. Peterson, N. Peterson, G. Stecher, M. Nei, S. Kumar, MEGA5: molecular evolutionary genetics analysis using Maximum likelihood, evolutionary distance, and Maximum parsimony methods, Mol. Biol. Evol. 28 (2011) 2731–2739, https://doi.org/10.1093/molbev/msr121.